

DOI: 10.1002/ ((please add manuscript number))

Article type: Paper

**Multifunctional Water Drop Energy Harvesting and Human Motion Sensor
Based on Flexible Dual-Mode Nanogenerator Incorporated with Polymer
Nanotubes**

Long-Biao Huang^{a,b}, Wei Xu^b, Chenghan Zhao^a, Yong-Liang Zhang^b, Kai-Leung Yung^c, Dongfeng Diao^d, Kin Hung Fung^b, Jianhua Hao^{b}*

Dr. L.-B. Huang, C. H. Zhao
a College of Physics and Optoelectronic Engineering, Shenzhen University,
Shenzhen, 518060, P. R. China

Dr. L.-B. Huang, Dr. W. Xu, Dr. Y.-L. Zhang, Dr. K. H. Fung, Prof. J. H. Hao
b Department of Applied Physics, The Hong Kong Polytechnic University, Hong
Kong, P. R. China
E-mail: jh.hao@polyu.edu.hk

Prof. K.-L. Yung
c Department of Industrial and Systems Engineering, The Hong Kong Polytechnic
University, Hong Kong, P. R. China

Prof. D. F. Diao
d Institute of Nanosurface Science and Engineering, Shenzhen University, Shenzhen
518060, P. R. China

Keywords: Triboelectric nanogenerator; Self-powered sensing; Mechanical energy
harvesting, Polymer nanotubes; Water drop

Abstract:

In the world of increasing energy consumption, nanogenerators have shown high
potential for energy harvesting and self-powered portable electronics. Here, flexible
and dual-mode triboelectric nanogenerator (TENG) combining both vertical contact-
separation and single electrical modes has been developed to convert environmental
mechanical energy into electricity with highly encapsulated and multifunctional

1 strategies. By introducing the polymer melt wetting technique, the polymer nanotubes
2
3 are fabricated on the surface of TENG, which provides self-cleaning and hydrophobic
4
5 features beneficial for water drop energy harvesting based on the device. For such
6
7 mechanical energy harvesting, the maximum output power and open-circuit voltage can
8
9 arrive at 0.025 mW and 41 V, respectively. By designing the dimensions of the device,
10
11 the dual-mode TENG is utilized as self-powered sensor to detect human body motion
12
13 such as phalanges movement of fingers. The fabricated dual-mode TENG promotes the
14
15 development of energy harvesting and self-powered human motion sensors for artificial
16
17 intelligent prosthetics, human kinematics and human body recovery treatment.
18
19
20
21
22
23
24
25
26

27 **1. Introduction**

28
29 The increased use of portable electronics products in the modern society has
30
31 aggravated energy consumption tremendously. To satisfy the energy demand for
32
33 portable electronics, a variety of approaches have been developed, such as solar
34
35 cells,[1-3] batteries,[4, 5] supercapacitors[6, 7] and nanogenerators.[8-10] Among
36
37 these advanced technologies, the nanogenerators based on piezoelectric or triboelectric
38
39 effect show great potential in a large amount of applications such as energy harvesting,
40
41 self-powered active sensors, blue energy harvesting and so on.[11-16]
42
43
44
45
46
47
48
49

50 Triboelectric nanogenerators (TENGs) originated from triboelectric and
51
52 electrostatic effects have shown great capability to harvest energy from ambient
53
54 mechanical motions and human body motions such as vibration, rotation, walking,
55
56 jumping, etc.[11-13, 17-19] Currently, four working modes of TENG have been
57
58
59
60
61
62
63
64
65

developed, including vertical contact-separation mode, lateral sliding mode, single-electrode mode and freestanding triboelectric-layer mode, showing distinct advantages to serve specific applications.[20-24] For instance, Wang's group has demonstrated lots of achievements of contact-separation mode TENGs which provide self-power capability for portable electronics that conventionally rely on batteries or capacitors.[13] Kim's group presented that the vertical contact-separation mode TENG based on graphene could drive commercial LCD, LED and EL display.[25] Additionally, single-electrode mode TENGs have been utilized to harvest the energy from water droplet by Wang's group.[23, 26, 27] Interestingly, Cao and Wang et al. demonstrate that TENGs with lateral sliding and freestanding modes can be utilized to harvest the energy of moving object or human body motions.[28]

Even though the rapid development of TENG is achieved for various applications, majority of TENGs are focused on the utilization of single working mode and hybridation of TENG and other energy harvesting device. [12, 13, 27] In order to simultaneously harvest different sources of ambient energy with higher efficiency, development of multimode TENG by integrating different single working mode into a single TENG device is highly desirable for conceiving novel applications. However, only a few attempts have been made to explore multimode nanogenerators for energy harvesting applications.[27, 28] It is noticeable that the reported dual-mode TENG without obvious encapsulation had already shown novel function as smart tactile sensor by combining single electrode and contact-separation modes.[28] Unfortunately, the research on multi-mode TENG is still in the incipient stage and hence there is much

room to deepen understanding of the device and endow it with synergistic multifunction by introducing novel nanomaterials. Therefore, further exploration of mutil-mode TENG can bring more benefits to both fundamental materials research and promising application of TENG. Inspiringly, polymers as essential and crucial materials of TENG have wide processing temperature range due to their thermal properties, which provides great potentials for the fabrication of multimode TENG. As summarized in our previous review, the distinctive, various, and tunable structures in 1D polymer nanomaterials such as nanotubes present nanointerfaces, high surface- to- volume ratio, and large surface area, which can improve the performance of energy devices.[29] Moreover, the polymer nanomaterials can be fabricated on the surface of polymer by various techniques. According to the wetting phenomena of polymer solution/melts in inorganic porous templates, Martin's group proved that polymer wetting is an effective technique to make polymer nanowires or nanotubes.[30, 31] Therefore, the combination of polymer wetting technique and manipulating polymer thermal processes may provide a route to investigate multimode TENG with the advantage of satisfied demand from different occasions.

Herein, we present a dual-mode TENG with vertical contact-separation and single electrode modes in a single TENG device. Comparing with previous report,[28] the encapsulation and functions of dual-mode TENG in our work have been significantly improved in a straightforward way. The formation of polymer nanotubes on the outer surface of TENG provides the device with superhydrophobic property, endowing TENG with additional self-cleaning function. The result shows that this dual-mode

TENG can be utilized for energy harvesting from ambient environment and the falling water drop. By changing the dimension of inner cavity in the device, the dual-mode TENG is capable of detecting the behaviors of human finger joints motions. This novel dual-mode device with versatile multifunctions promotes the development of TENG in energy harvesting from environment,[23, 26, 27, 32] and also demonstrates the potentials for self-powered and self-cleaning human motion sensors.

2. Results and discussions

In order to fabricate highly encapsulated and multifunctional dual-mode TENG, the polyethylene (PE) films, Polytetrafluoroethylene (PTFE) film, aluminum film and porous alumina templates were assembled as shown in **Figure 1a**. During heating of the assembled specimen in the oven at 120 °C for about 30 mins, the PE films arrive at above melting temperature and start to melt, resulting in the encapsulation and adhesion between top and bottom PE films. After cooling, the enclosed PTFE by PE films was easily peeled off due to the non-adhesive property between PE and PTFE films, leading to the construction of an inner cavity. In the cavity, the Al film was thermal-bonded on the surface of PE film, serving as the electrode and one contact materials. The inner surface of PE film performs as another contact material of contact separation mode and its morphology was investigated by SEM as shown in **Figure 1b**. It is found that there is significantly nanopatterned feature on the inner surface, which was duplicated from PTFE surface. On the other hand, the PE melts also lead to the formation of nanotubes on the outer surface of PE films after etching the porous alumina templates for single

electrode mode. As shown in **Figure 1c**, the SEM image confirms that large amount of PE nanotubes with an average length and diameter of 30 μm and 200 nm, respectively, have been successfully fabricated on the outer surface of PE film. The results are consistent with the earlier report.[33] The formation mechanism of these PE nanotubes is attributed to the polymer melt wetting phenomenon in the porous materials.[30, 31] The PE melt with lower surface energy can be absorbed into nanochannels of porous alumina template due to the surface energy difference between PE melt and porous alumina template which has higher surface energy. Therefore, after cooling and removing the porous alumina template by NaOH solution, the PE nanotubes are released from templates and kept on the surface. These nanotubes can provide the PE film surface with hydrophobic property.[33, 34] As shown in the inset image of **Figure 1d**, the contact angle of the prepared PE films can reach up to 156°, indicating their great super-hydrophobic ability. Based on the structural design here, vertical contact-separation and single electrode modes are easily integrated into a single device as shown in **Figure 1a**. The vertical contact-separation mode in PE cavity consists of two parts, including PE film and aluminum foil which perform as two contact materials, as shown in blue rectangle. The single electrode mode is shown in red rectangle, which is the PE film thermal-bonded on the surface of aluminum film. The aluminum film serves as an electrode for both modes. The whole fabrication processes show an improvement in easier fabrication and more highly capsulation compared to previously reported work.

[28]

The working principles of this dual-mode TENG are schematically illustrated as shown in **Figure 2** (contact-separation mode: **2a**; single-electrode mode: **2b**). Under external mechanical forces such as flap, water drop or wind, the inner surface of PE film with nanopatterned feature could contact and separate with Al electrode as shown in **Figure 2a**. According to the differences of triboelectric polarities in varied tribo-materials,[11] the positive charges on the Al electrode and negative charges on the surface of PE film are generated after the separation between Al electrode and PE film, leading to the electrical difference between two Al electrodes. Therefore, electrons can flow between Al electrodes as shown in (**Figure 2a**, i). When the PE film contacts with Al electrode again (**Figure 2a**, ii), the opposite electrical difference created between Al electrodes results in an opposite instantaneous current. In response to the periodically contact and separation between PE film and Al electrode (**Figure 2a**, iii and iv), the instantaneous alternating current is created. For single-electrode mode, when water drop from the sky/pipes falls towards the surface of PE film (**Figure 2b**, i), the water drop could contact and spread on hydrophobic surface of PE film (**Figure 2b**, ii and iii). Although it has been deionized, the pure DI water still has equilibrium between OH^- and H^+ due to the dissociation of water molecular. The processes of spreading and contacting between water drop and PE film will therefore lead to the generation of electric double layer (EDL) at the water drop-hydrophobic surface based on triboelectricity effect. When the water drop is rebounded from the surface of PE film due to its hydrophobic property, the jumping water drop will carry some net positive charges and the PE hydrophobic surface could be negatively charged attributed to the

preferential absorption of hydroxide ions from water droplet. Consequently, an electric potential difference is created between Al electrode and PE film and lead to the flowing of electrons from Al electrode to ground to create an instantaneous negative current (**Figure 2b, iv**). [35] Due to the insulation property of PE, the triboelectric charge could be maintained on the surface until contacting with another water droplet. When another water droplet falls and contacts with the negative charged area of hydrophobic film, the negative charges will attract H^+ from water and lead to the formation of EDL and the flowing back of electrons from ground to electrodes (**Figure 2b, v, vi, and vii**). The subsequent separation of the water drop can induce the opposite electron flowing (**Figure 2b, viii**). Through the continuously water drops, alternating current is created.

For both single electrode and contact-separation modes, the overall voltage difference between electrodes can be given by: [36, 37]

$$V = -\frac{Q}{C} (d + x(t)) + \frac{ax(t)}{c_0} \quad (1)$$

where c_0 is the permittivity of vacuum, a is the average surface charge density of contact materials in vertical contact-separation and single electrode modes, S is the area size of contact area in device, Q is the transferred charges in whole working process, x is the separation distance in the PE cavity. Therefore, the open-circuit voltage V_{oc} from the polarized triboelectric charges and short-circuit charges Q_{sc} are $ax(t)/c_0$ and $Sax(t)/(d+x(t))$, respectively, for both single electrode and contact-separation modes.

1 preferential absorption of hydroxide ions from water droplet. Consequently, an electric
2
3 potential difference is created between Al electrode and PE film and lead to the flowing
4
5 of electrons from Al electrode to ground to create an instantaneous negative current
6
7
8
9 (**Figure 2b, iv**).[35] Due to the insulation property of PE, the triboelectric charge could
10
11 be maintained on the surface until contacting with another water droplet. When another
12
13

The TENG device with the size of $40 \times 40 \times 2$ mm was fabricated to evaluate the performance of device under vertical contact-separation mode as shown in **Figure 3** under ~ 2 N force in ambitious condition. The results show that the V_{oc} and I_{sc} of basic TENG device are measured to be about 41 V and 1.3 μ A, respectively, as shown in **Figure 3a** and **3b**. The relative dependence of the output voltage and current across the resistance of external load is shown in **Figure 3c**. The trends of output voltage and output current are in accordance with previous literatures,[38, 39] which means that the output voltage increases and output current decreases with the increment of resistance. The maximum electric power is around 0.025 mW at a load resistance of 10 Mn. The prepared TENG working in vertical contact-separation mode could simultaneously lighten 5 commercial red LEDs as shown in the inset of **Figure 3d**, showing its capability of harvesting mechanical energy from external environment. Besides, the figure-of-merits (FOM) of device was also calculated according to the literature.[37] The maximum structural FOMs and materials FOMs are 0.987 and 306.25 μ C²/m, respectively.

Besides contact-separation mode, the as-prepared TENG could also work simultaneously under dual-mode for harvesting energies. The DI water drop with volume of $\sim 60 \mu$ L was dripped to the superhydrophobic surface on the single electrode TENG side and the whole device was fixed at a tilted angle of 45° as shown in **Figure 4a**. [23, 32] The initial height between water drop and superhydrophobic surface was set as 25 cm.[32] Due to the hydrophobic properties (CA, $\sim 156^\circ$) of PE film, the water drop could be easily rounded from surface of the device. The V_{oc} and I_{sc} were measured

to evaluate the electric output performance of TENG in harvesting energies from water drop. **Figure 4b** and **4c** present the typical output curves of V_{oc} and I_{sc} generated from dual-mode TENG. It is found that the V_{oc} and I_{sc} are approximately 4.0 V and 71 nA, respectively. As shown in **Figure 4d**, the output current keeps a slight change at maximum value of about 70 nA, and then decreases with the increment of external resistance. The output voltage shows an opposite change trend that the output voltage increases with the increment of external resistance and achieves at the maximum value of around 4.1 V. The maximum output power of 0.14 μ W is achieved at an external load resistance of 10 Mn. The generated power can enlighten LED as shown in the inset photography of **Figure 4e**. To illustrate the working mechanism more clearly, V_{oc} of single-electrode mode TENG without integrating contact-separation mode was measured under identical condition as shown in **Figure 4f**, in which V_{oc} could reach up around ~ 0.68 V. By contrast, dual-mode TENG shows higher V_{oc} with 4.1 V. As previously mentioned, the dual-mode TENG was fabricated with integration of vertical contact-separation mode and single electrode mode into single TENG device. Therefore, the higher energy output might be attributed to the co-existence of different working modes and their synthetic effect. Due to the contact-electrification between the nanopatterned PE film and Al electrode as well as the electrostatic effect, the superhydrophobic surface of single-electrode mode is positively charged. Therefore, the contact of DI water drop with hydrophobic surface of PE film will drive electrons flow from Al to the ground.[23] When the water drop rebounds from superhydrophobic surface of dual-mode TENG, electrons flow from ground to Al. During the same

processes, the gravity of DI water drop causes the contact between the nanopatterned PE film and Al electrode, resulting in the electrons flow from Al electrode to ground for attaining an equilibrium state. When DI water drop is pushed away by superhydrophobic surface, the PE film and Al electrode are separated, and opposite electrons flow is created. At the same time, it is very hard to avoid the external contamination from ambient environment such as dusts for practical application. Superhydrophobic of polymer micropattern provides self-cleaning property to the TENGs, as shown in **Figure 4g-i**, in which the dust on the surface of device could be self-cleaned by the water drop. To simulate the practical application, the shower nozzle was utilized to produce water drops which impact the TENGs. As shown in **Figure 4g-ii**, the original TENGs without dust contamination have about 8.1 V of V_{oc} under the impact of water drops. After introducing slight contamination by dusts, the output performance of TENG experiences two stages. At the first stage, the dust on the surface of TENGs lead to the low V_{oc} . After that, the V_{oc} can automatically recovery to the previous value during the water drop energy harvesting process. At the first stage, the decrement of output performance could be attributed to the following two factors. Firstly, the dusts on the surface of device can cause the loss of contact area between waterdrop and PE surface, which has strong negative effect on the formation of EDL, leading to the decrement of output performance of single-electrode TENG. Secondly, the weight of dusts reduces the gap between PE film and Al electrode, which has large influence on the performance of contact-separation mode TENG. Accompanying with the removing of the dusts and the self-cleaning of the device surface by water drops,

V_{oc} of the device can recovery to ~ 8.1 V, which is almost indential with that from original device. Therefore, the dual-mode TENG with self-cleaning feature shows a capability for harvesting the energy of water drop.

The as-prepared dual-mode TENG has superhydrophobic surface at both sides of the device which has the capability for self-cleaning application as shown in **Figure 4g-i**. Considering the human body motion detector usually contacts with skin with sweat and dusty, it is feasible to develop our dual-mode TENG with self-cleaning function as the self-powered human motion sensor. By simply designing the size of device, the dual-mode TENG with the inner cavity dimension of $30 \times 5 \times 2$ mm is utilized to detect the motions of index, middle, ring and little fingers. As shown in **Figure 5a**, the index finger presents maximum voltage about 320 mV at 90° bending angle, while under identical bending condition little finger shows minimum voltage value of 110 mV, middle finger and ring finger show 230 mV and 180 mV, respectively. By changing different bending angle of index finger, the detected voltage signals indicate that the increment of index finger bending angle leads to an increase in voltage signal as presented in **Figure 5b**. At low bending angle from 15° to 45° , the voltage increases slightly from 20 mV to 51 mV, while the voltage remarkably increases from 51 mV to 320 mV with bending angle's increment from 45° to 90° . The variation in electric signals for different bending angles in **Figure 5b** would be attributed to several factors, such as the change of contact area between PE film and Al electrode in vertical contact-separation mode, and the change in capacitive coupling between human skin and device electrode in single-electrode mode.

Firstly, the bending of device will lead to the contact and separation of PE film and Al electrode at finger joint.[40] At high bending angles, the bending behavior of finger will lead to more contact area between PE film and Al electrode in TENG. As the electrical output of TENG is based on the charge transfer between polymer and electrodes, larger contact areas between polymer and electrodes could lead to higher electrical signals.

Secondary, the epidermis conductive characteristics lead to the capacitive coupling between AC conductors and electrical equipment for single electrode mode.[41, 42] The stacked layers of Al electrode, PE film and epidermis create a capacitive system. The variable capacitor (C_{FD}) between device and epidermis results in the change in voltage intensity of Al electrode. C_{FD} is represented as

$$C_{FD} = \int_0^l \epsilon_0 \frac{w}{d} dl, \quad (2)$$

where ϵ_0 is the permittivity of vacuum, w is the width of device, d is the distance between electrode and epidermis, and l is the length across the epidermis surface. As shown in **Figure 5b**, the distance between epidermis and Al electrode (d) decreases along when increasing the bending angle. The decreased d can result in the increment of capacitance, and further lead to the higher V_{oc} in the measurement.[42] Under cooperative operation of vertical contact-separation mode and single electrode modes, the as-prepared dual-mode TENG can be utilized to detect human body motion and obviously show distinct signals for different finger bending. Consequently, the presented results might be potential for further application in artificial intelligent prosthetics, human kinematics and human body recovery treatment.[40]

4. Experimental Section

Materials: Low density PE films were purchased from Hualong Materials Co., Ltd. Porous alumina template was purchased from GE Whatman Co., Ltd. with a through-hole nanochannel diameter of 200 nm and 60 μm thickness. Sodium hydroxide, acetone, ethanol and other chemicals were purchased from Sigma-Aldrich and used without further purification.

Fabrication of dual-mode TENG with super-hydrophobic surface: The PE films, PTFE plate (2 mm), aluminum film and porous alumina templates were assembled as shown in **Figure 1a** and heated in an oven of 120 $^{\circ}\text{C}$ for about 30 mins. After cooling to room temperature, NaOH solution was utilized to etch porous alumina template as previous studies.[33, 43] Then, the PE films with nanotube patterned surface were formed and rinsed with deionized water and absolute ethanol, respectively. After subsequently removing the PTFE film, an inner cavity was formed between PE and Al films. Consequently, a dual-mode TENG possessing vertical contact-separation and single-electrode modes, was achieved, where the alumina film functions as electrode to the dual-mode TENG. The prepared specimen sizes for energy harvesting and motion sensor are 40 \times 40 mm and 30 \times 5 mm, respectively. More details regarding the fabrication process of the dual-mode TENG are schematically illustrated in **Figure 1a**.

Characterizations: The surface morphology of PE film was investigated using scanning electron microscopy (SEM, JEOL Model JSM-6490) under accelerating voltage of 5 kV. Static water contact-angle measurements were carried out using a Rame-hart Model-F1 Standard Gonimeter with Drop image Advanced 2.1 at room temperature. 3

1 μl deionized (DI) water was placed on the surface of PE film for contact angle
2
3
4 measurement. The contact angle was determined by fitting a Young-Laplace curve
5
6 around the water drop. The kinetic contact of water droplet was measured by Kruss
7
8 DSA100 at room temperature. The open-circuit voltage (V_{oc}) and short-circuit current
9
10 (I_{sc}) were measured by LeCroy Wave Runner Oscilloscope (44MXI) with probe
11
12 resistance value of 10 Mn and SR570 low noise current amplifier (Stanford Research
13
14 System), following literatures.[44-46]
15
16
17
18
19
20
21
22
23
24

25 **Supporting Information**

26
27 Supporting Information is available from the Wiley Online Library or from the
28
29 author.
30
31
32
33

34 **Acknowledgements**

35
36
37 The research is financially supported by the grants from Science Foundation of
38
39 Guangdong Province (Grand No.2018A0303130060 and 2019A1515011566), the
40
41 Science and Technology Innovation Commission of Shenzhen (Grant
42
43 No.JCYJ20170818101245583), Natural Science Foundation of China (Grant No.
44
45 51973119), Research Grants Council of Hong Kong (GRF No. PolyU 153025/19P),
46
47 PolyU Internal Grant (1-ZVGH).
48
49
50
51
52
53

54 Received: ((will be filled in by the editorial staff))

55 Revised: ((will be filled in by the editorial staff))

56 Published online: ((will be filled in by the editorial staff))
57
58
59
60
61
62
63
64
65

Reference

- [1] M.Z. Liu, M.B. Johnston, H.J. Snaith, *Nature*, 501 (2013) 395-+.
- [2] B. Oregan, M. Gratzel, *Nature*, 353 (1991) 737-740.
- [3] W.J. Jie, F.G. Zheng, J.H. Hao, *Appl Phys Lett*, 103 (2013). 233111
- [4] C.K. Chan, H.L. Peng, G. Liu, K. McIlwrath, X.F. Zhang, R.A. Huggins, Y. Cui, *Nat Nanotechnol*, 3 (2008) 31-35.
- [5] H. Wu, G. Chan, J.W. Choi, I. Ryu, Y. Yao, M.T. McDowell, S.W. Lee, A. Jackson, Y. Yang, L.B. Hu, Y. Cui, *Nat Nanotechnol*, 7 (2012) 309-314.
- [6] L.L. Zhang, X.S. Zhao, *Chem Soc Rev*, 38 (2009) 2520-2531.
- [7] D.N. Futaba, K. Hata, T. Yamada, T. Hiraoka, Y. Hayamizu, Y. Kakudate, O. Tanaike, H. Hatori, M. Yumura, S. Iijima, *Nat Mater*, 5 (2006) 987-994.
- [8] X.D. Wang, J.H. Song, J. Liu, Z.L. Wang, *Science*, 316 (2007) 102-105.
- [9] Z.L. Wang, J.H. Song, *Science*, 312 (2006) 242-246.
- [10] F.R. Fan, Z.Q. Tian, Z.L. Wang, *Nano Energy*, 1 (2012) 328-334.
- [11] G. Cheng, Z.H. Lin, L. Lin, Z.L. Du, Z.L. Wang, *Acs Nano*, 7 (2013) 7383-7391.
- [12] Z.L. Wang, *Advanced Materials*, 24 (2012) 280-285.
- [13] Z.L. Wang, J. Chen, L. Lin, *Energ Environ Sci*, 8 (2015) 2250-2282.
- [14] J. Chen, J. Yang, Z.L. Li, X. Fan, Y.L. Zi, Q.S. Jing, H.Y. Guo, Z. Wen, K.C. Pradel, S.M. Niu, Z.L. Wang, *Acs Nano*, 9 (2015) 3324-3331.
- [15] Z. Wen, H. Guo, Y. Zi, M.-H. Yeh, X. Wang, J. Deng, J. Wang, S. Li, C. Hu, L. Zhu, *Acs Nano*, 10 (2016), 6526-6534.
- [16] W. Xu, M.C. Wong, J.H. Hao, *Nano Energy*, 55 (2019) 203-215.
- [17] Z.L. Wang, *Mater Today*, 2 (2017), 74-82.
- [18] C.K. Jeong, K.M. Baek, S.M. Niu, T.W. Nam, Y.H. Hur, D.Y. Park, G.T. Hwang, M. Byun, Z.L. Wang, Y.S. Jung, K.J. Lee, *Nano Lett*, 14 (2014) 7031-7038.
- [19] H. Fang, X. Wang, Q. Li, D. Peng, Q. Yan, C. Pan, *Adv Energy Mater*, (2016) 1600829.
- [20] Y. Yang, Y.S. Zhou, H.L. Zhang, Y. Liu, S.M. Lee, Z.L. Wang, *Advanced Materials*, 25 (2013) 6594-6601.

- [21] S.H. Wang, L. Lin, Y.N. Xie, Q.S. Jing, S.M. Niu, Z.L. Wang, Nano Lett, 13 (2013) 2226-2233.
- [22] G. Zhu, C.F. Pan, W.X. Guo, C.Y. Chen, Y.S. Zhou, R.M. Yu, Z.L. Wang, Nano Lett, 12 (2012) 4960-4965.
- [23] Z.H. Lin, G. Cheng, S. Lee, K.C. Pradel, Z.L. Wang, Advanced Materials, 26 (2014) 4690-+.
- [24] Z.L. Wang, Acs Nano, 7 (2013) 9533-9557.
- [25] S. Kim, M.K. Gupta, K.Y. Lee, A. Sohn, T.Y. Kim, K.S. Shin, D. Kim, S.K. Kim, K.H. Lee, H.J. Shin, D.W. Kim, S.W. Kim, Advanced Materials, 26 (2014) 3918-3925.
- [26] H.R. Zhu, W. Tang, C.Z. Gao, Y. Han, T. Li, X. Cao, Z.L. Wang, Nano Energy, 14 (2015) 193-200.
- [27] Z.H. Lin, G. Cheng, W.Z. Wu, K.C. Pradel, Z.L. Wang, Acs Nano, 8 (2014) 6440-6448.
- [28] T. Li, J. Zou. F. X, M. Zhang, X. Cao, N. Wang, Z.L. Wang, ACS Nano, 11 (2017) 3950-3956.
- [29] L.B. Huang, W. Xu, J.H. Hao, Small, 13 (2017), 1701820.
- [30] M. Steinhart, J.H. Wendorff, A. Greiner, R.B. Wehrspohn, K. Nielsch, J. Schilling, J. Choi, U. Gosele, Science, 296 (2002) 1997-1997.
- [31] M. Steinhart, R.B. Wehrspohn, U. Gosele, J.H. Wendorff, Angewandte Chemie-international Edition, 43 (2004) 1334-1344.
- [32] S.B. Jeon, D. Kim, G.W. Yoon, J.B. Yoon, Y.K. Choi, Nano Energy, 12 (2015) 636-645.
- [33] L.B. Huang, Y. Zhou, S.T. Han, Y. Yan, L. Zhou, W. Chen, P. Zhou, X. Chen, V. Roy, Small, 10 (2014), 4645-4650.
- [34] W. Tian, Y. Xu, L. Huang, K.-L. Yung, Y. Xie, W. Chen, Nanoscale, 3 (2011) 5147-5155.
- [35] D. Choi, H. Lee, D.J. Im, I.S. Kang, G. Lim, D.S. Kim, K.H. Kang, Scientific Reports, 3 (2013) 2037.

- [36] Y. Zi, J. Wang, S. Wang, S. Li, Z. Wen, H. Guo, Z.L. Wang, *Nature Communications*, 7 (2016), 10987.
- [37] Y.L. Zi, S.M. Niu, J. Wang, Z. Wen, W. Tang, Z.L. Wang, *Nat Commun*, 6 (2015), 8376.
- [38] W. Xu, M.C. Wong, Q.Y. Guo, T.Z. Jia, J.H. Hao, *J Mater Chem A*, 7 (2019) 16267-16276.
- [39] M.C. Wong, W. Xu, J.H. Hao, *Adv Funct Mater*, 29 (2019), 1904090.
- [40] G. Wu, F.C. Van der Helm, H.D. Veeger, M. Makhsous, P. Van Roy, C. Anglin, J. Nagels, A.R. Karduna, K. McQuade, X. Wang, *Journal of biomechanics*, 38 (2005) 981-992.
- [41] D.T. Lykken, P.H. Venables, *Psychophysiology*, 8 (1971) 656-672.
- [42] L. Dhakar, P. Pitchappa, F.E.H. Tay, C. Lee, *Nano Energy*, 19 (2016) 532-540.
- [43] L. Huang, Z. Xu, X.-F. Chen, W. Tian, S.-T. Han, Y. Zhou, J.-J. Xu, X.-B. Yang, V.A. Roy, *ACS applied materials & interfaces*, 15 (2014) 11874-11881.
- [44] L.B. Huang, G.X. Bai, M.C. Wong, Z.B. Yang, W. Xu, J.H. Hao, *Advanced Materials*, 28 (2016) 2744-2751.
- [45] L.B. Huang, W. Xu, G.X. Bai, M.C. Wong, Z.B. Yang, J.H. Hao, *Nano Energy*, 30 (2016) 36-42.
- [46] W. Xu, L.B. Huang, M.C. Wong, L. Chen, G. Bai, J. Hao, *Advanced Energy Materials*, 7 (2017) 1601529.

Figure lists

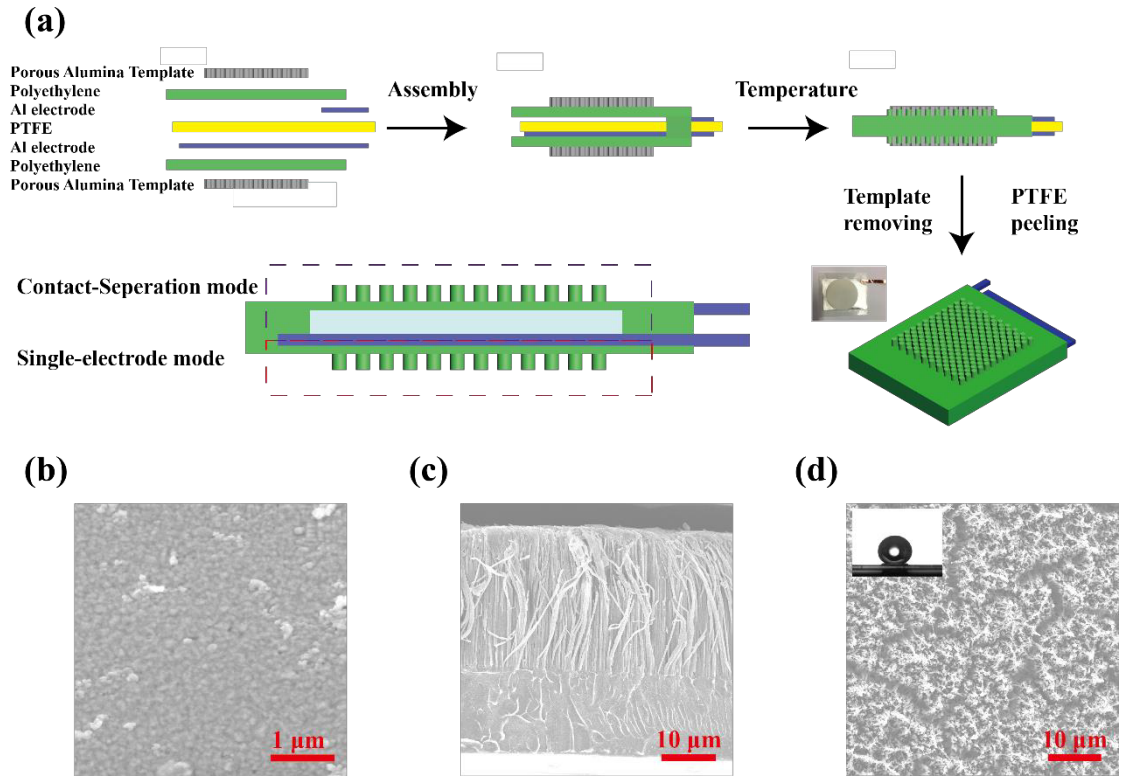


Figure 1. (a) Schematical illustration of fabrication processes of dual-mode triboelectric nanogenerator with real device in the inset. (b) SEM image of surface morphology of PE film inside the cavity. (c) Cross-sectional SEM image of PE film. (d) Top-view SEM image of PE film outer surface with contact angle (156°) image.

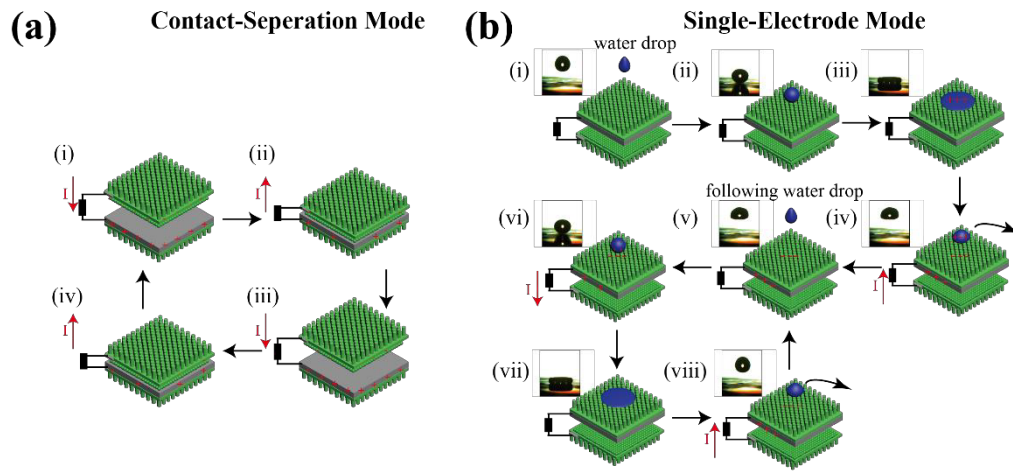


Figure 2. Schematically illustration of working principle of contact-separation mode (a) and single-electrode mode (b). Inset shows the ultrafast rebound images of water drop on the surface of PE film with nanotubes.

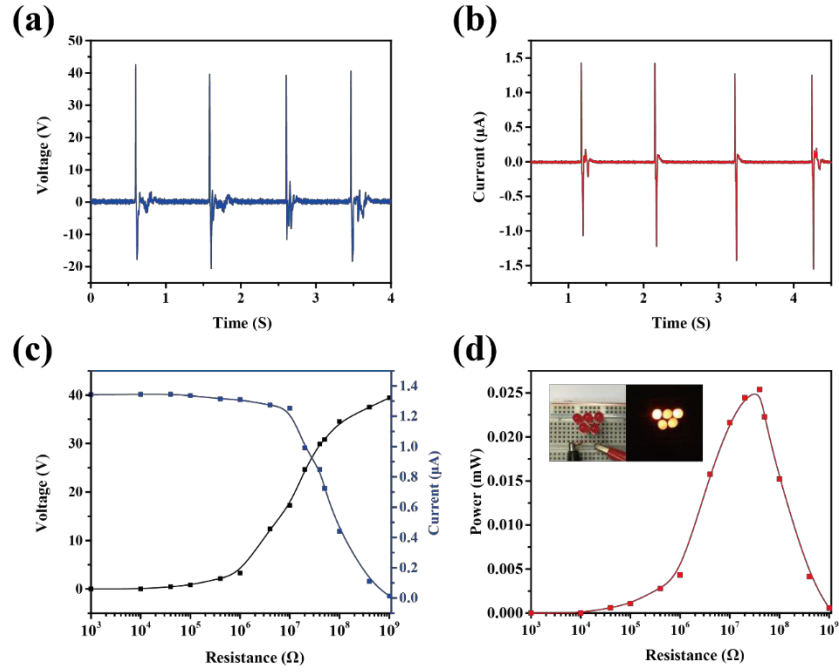


Figure 3. (a) and (b) The open-circuit voltage and short-circuit current of TENG with 2 mm height in the cavity in vertical contact-separation mode. (c) Dependences of open-circuit voltage and short-circuit current across the resistance of external load. (d) Dependence of output power on the resistance of external load. Inset photograph shows red LEDs without external circuit components.

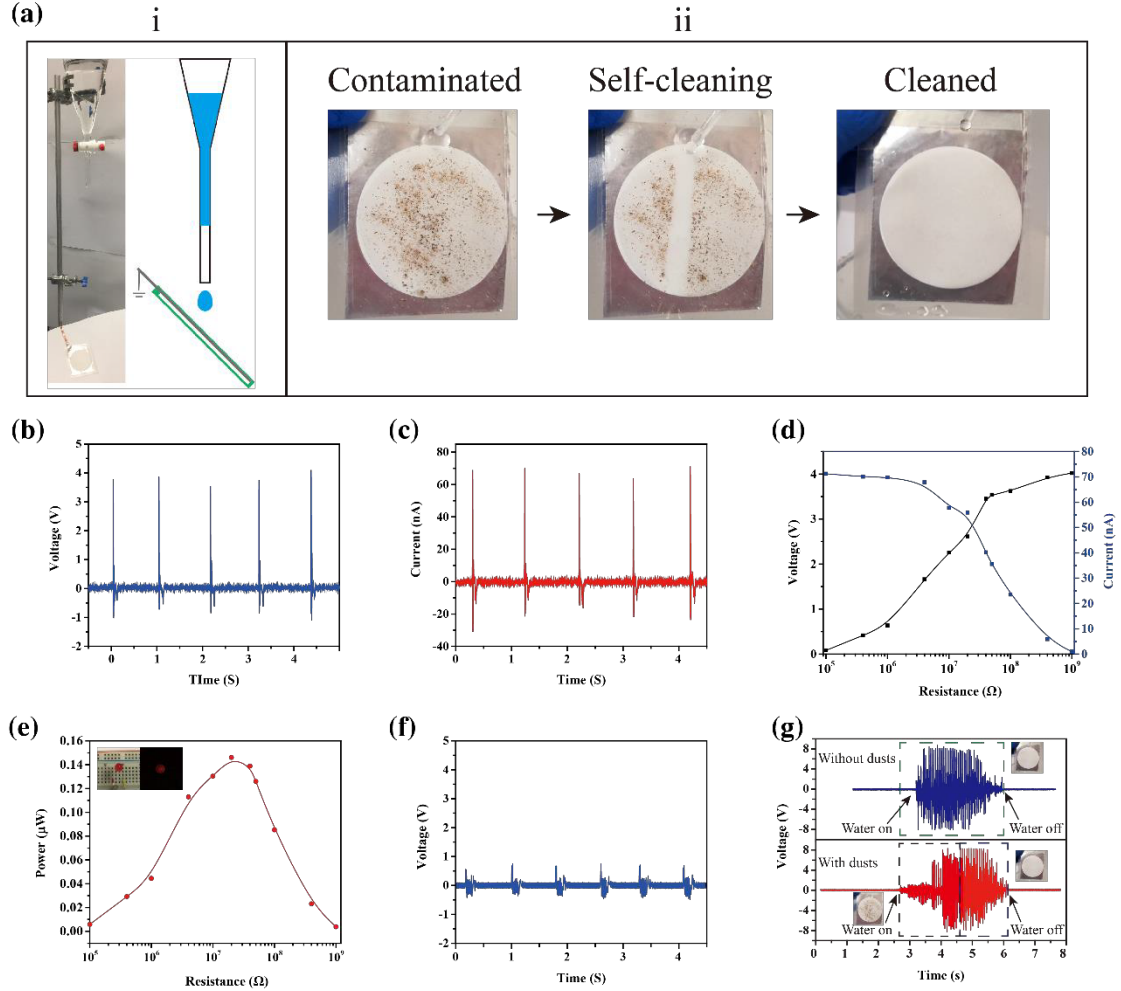


Figure 4. (a) i: The set-up for energy harvesting from water drop; ii: self-cleanability of dual-mode triboelectric nanogenerator before and after washing by water droplet. (b) and (c) The open-circuit voltage and short-circuit current of dual-mode triboelectric nanogenerator driven by water drop. (d) The open-circuit voltage and short-circuit current on the different resistance of external load. (e) Dependence of output power on the resistance of external load. Inset photograph shows red LEDs without external circuit components. (f) The open-circuit voltage of triboelectric nanogenerator working only in single-electrode mode. (g) The open-circuit voltage of original device and slight contaminated device under shower nozzle.

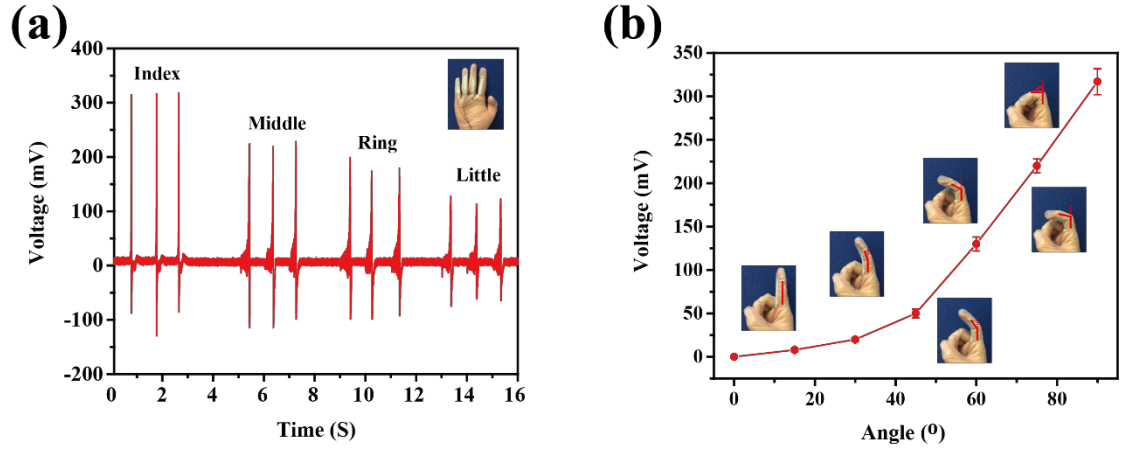


Figure 5. Application of TENG as self-powered sensor to detect finger joint motion.

(a) Open-circuit voltage responses at different bending angles. (b) Open-circuit voltage responses at different bending rates.

Table of Content:

A novel and flexible TENG with the integration of both vertical contact-separation and single electrical modes has been developed. The hydrophobic properties originated from the polymer nanotubes on the device's surface provide the self-cleaning function to TENG, which is more suitable to harvest the energy from water drop. By designing the dimension of device, the dual-mode TENG has been utilized as self-powered sensor to detect human motion such as phalanges motion of fingers.

Long-Biao Huang, Wei Xu, Chenghan Zhao, Yong-Liang Zhang, Kai-Leung Yung, Dongfeng Diao, Kin Hung Fung, Jianhua Hao*

Multifunctional Water Drop Energy Harvesting and Human Motion Sensor Based on Flexible Dual-Mode Nanogenerator Incorporated with Polymer Nanotubes

ToC figure

